Bergvesenet

Postboks 3021, N-7441 Trondheim

Rapportarkivet

Bergvesenet rapport nr	Intern Journal nr	Internt arkiv nr	Rapport lokalisering	Gradering
6944				

Kommer fra arkiv	Ekstern rapport nr	Oversendt fra	Fortrolig pga	Fortrolig fra dato
Grong Gruber AS		F.M. Vokes		

Tittel

"Pseudostratigraphy" and Thrusting in Relation to the Structural Evolution of the Joma Ore-Body, North Trøndelag, Norway

Forfatter	Dato	År	Bedrift (Oppdragsgiver og/eller oppdragstaker)
Marshall, Brian	nov	1990	Grong Gruber AS

Kommune	Fylke	Bergdistrikt	1: 50 000 kartblad	1: 250 000 kartblad
Røyrvik	Nord-Trøndelag		19241	Grong

Fagområde	Dokument type	Forekomster (forekomst, gruvefelt, undersøkelsesfelt)
Geologi		Jomaforekomsten

Råstoffgruppe	Råstofftype
Malm/metall	Cu,Zn

Sammendrag, innholdsfortegnelse eller innholdsbeskrivelse

Mine-scale inversion is supported by orebody zonation and the relative position of ore layer and feeder system. Mesoscale streuctureal data require regionallytwo major periodes, D2 and D3, and one minor periode D1. At the end of D1, pseudostratigraphy og the thrust-disrupted ore system occupied the lower limb og an E-closing regionally developed antiformal anticline. Folding and sliding during D2 resulted in the further disrupted ore system being inverted and occupying the lower limb of a large-scale, E-closing, F2 antiform.

Artikkel i Ore Geology Reviews, 5 (1990) 175-210

Ore Geology Reviews, 5 (1990) 175–210
Elsevier Science Publishers B.V., Amsterdam — Printed in The Netherlands

With Compliments

Brian

"Pseudostratigraphy" and Thrusting in Relation to the Structural Evolution of the Joma Ore-Body, North Trøndelag, Norway

BRIAN MARSHALL

Department of Applied Geology, University of Technology, Sydney, P.O. Box 123, Broadway, N.S.W. 2007 (Australia)

(Received March 2, 1988; revised and accepted April 26, 1989)

Abstract

Marshall, B., 1990. "Pseudostratigraphy" and thrusting in relation to the structural evolution of the Joma orebody, North Trøndelag, Norway, *Ore Geol. Rev.*, 5: 175–210.

Joma Mine exploits a stratiform Cu–Zn volcanic-associated massive sulphide deposit within the Norwegian Caledonides. The ore layer overlies an inferred feeder system hosted by mafic metavolcanites within the grossly inverted stratigraphy of the Leipik Nappe. Mine-scale inversion is supported by orebody zonation and the relative position of ore layer and feeder system.

Mesoscale structural data from regionally distributed quartz-rich phyllites require two major periods (D_2 and D_3) and one minor period (D_4) of deformation. D_2 generated a transposition foliation containing an elongation lineation essentially co-linear with F_2 hinge lines. D_3 formed a NW-dipping crenulation foliation as hinge surface to SW-plunging F_3 folds. Before F_3, D_2 linear data probably trended NW in the shallowly W-dipping transposition foliation. D_4 formed minor kinkbands. Mesoscale data from the ore layer affirm the deformation sequence, but also suggest a D_1 thrusting and folding event. F_2 vergence and facing at regional and mine scales further support D_1.

The ore-layer sequence varies between and, less commonly, within layers, and lacks consistent polarity. This variable sequence is ascribed to D_1 and D_2 thrusting, folding and sliding, and is herein termed "pseudostratigraphy". The existence of level-scale pseudostratigraphy contrasts with preservation of gross relationships at mine scale, and places limitations on the dimensions and consequences of D_1 and D_2 structures.

At the end of D_1, pseudostratigraphy of the thrust-disrupted ore system occupied the lower limb of an E-closing regionally developed antiformal anticline. Folding and sliding during D_2 resulted in the further disrupted ore system being inverted and occupying the lower limb of a large-scale, E-closing, F_2 antiform. In D_3, the inverted ore layer occupied and was slightly S of the broad hinge zone of the regionally developed NE-closing Joma Synform; its present arcuate geometry reflects this. D_4 had little influence on the structural evolution of the orebody.

Introduction

Joma Mine is situated some 250 km NE of Trondheim close to the Swedish border in the Grong district of Norway (Fig. 1). The mine exploits a Cu–Zn orebody which is one of numerous stratabound and, as is the case with Joma, stratiform massive sulphide deposits principally within the Norwegian portion of the Caledonides. The geological setting of these deposits, their deposit-type classification, and their relationship to other types of volcanic-associated massive sulphide orebodies have been discussed in many articles (e.g. Vokes, 1976; Bjørlykke et al., 1979, 1980; Klau and Large,

0169-1368/90/$03.50

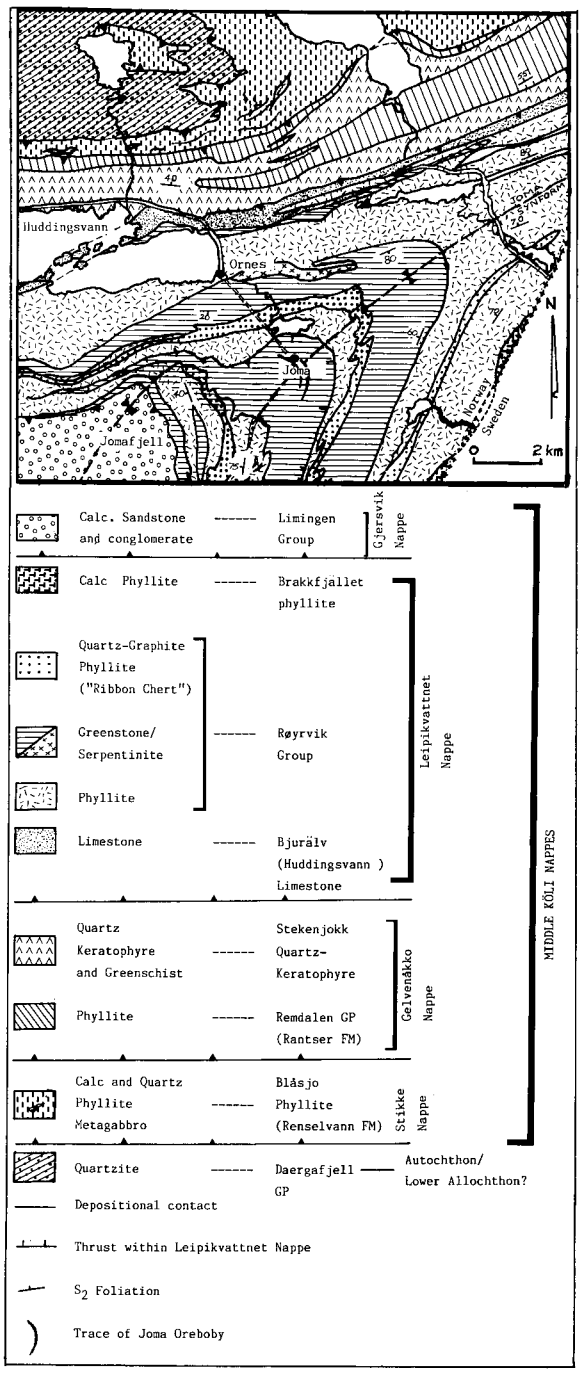

Fig. 2. Geological map of the Joma Mine area, showing the main stratigraphic divisions, the nappes and the Joma Synform. Geology is based on Kollung (1979) and Reinsbakken and Stephens (1986).

though Roberts (1979) and Kollung (1979) recognized multi-event deformation histories, complex event sequences have been reported from adjacent areas in Sweden (Trouw, 1973; Sjöstrand, 1978), Olsen (1980) interpreted the geometry of the Joma deposit in terms of two main events (Table 1). Nevertheless, to accommodate the possibility of an earlier ("pre-D_1") event in the Joma region, consistent with that found in some adjacent areas, the two main mesoscale events in this paper are designated D_2 and D_3.

Olsen (1980) concluded that the orebody exhibits a well-defined stratigraphy (Table 2) and lies in an inverted position (Fig. 3). His belief in stratigraphic inversion rested on:

(a) the albite rock and chlorite schist being a sub-ore alteration assemblage associated with the feeder system;

(b) zonation in volcanic-associated massive sulphide deposits (Franklin et al., 1981; Marshall and Gilligan, 1987) being best satisfied by chalcopyrite–pyrrhotite ore underlying chalcopyrite–sphalerite–pyrite ore; and

(c) Kollung's (1979) arguments for nappe-scale inversion.

Based on the metavolcanite geochemistry, Olsen (1980) suggested that the Joma deposit formed in a back-arc basinal environment.

TABLE 1

Deformational history of the Joma Orebody (after Olsen, 1980)

Event	Description
D_1^*	Represented by isoclinal folds (F_1) with a SE-trending axial direction and amplitudes up to a few meters, that deform wallrocks as well as ore layers - larger amplitudes of several hundred meters are inferred - the event was associated with thrusting and nappe development
D_2^*	The main deformation developed open to tight, asymmetric crenulation folds trending nearly at right angles to the F_1 axis

*Respectively equated with D_2 and D_3 in the present article.

to the mine, to outline the rock sequence in different parts of the orebody within the context of Olsen's stratigraphy, and to discuss the implications of these data for the internal structure and external morphology of the orebody. In turn, this will provide an overview of the mechanical behaviour of ore and hostrocks in convergent tectonic terrains involving thrusting and nappe formation.

Structural relationships

Surface structure

Investigation of the surface structure by Odling (1984), together with limited traversing by the present author, provided a framework for evaluating the mine structure. Of the main rock units (Fig. 2), the quartzose phyllites yielded the most informative structural data. The principal surface is a transposition foliation (S_{0-2}) comprising a discontinuous primary layering (S_0) and a penetrative, non-crenulate cleavage or low grade schistosity (S_2). S_{0-2} carries a mineral lineation (L_m) and is overprinted by a crenulation foliation (S_3; see Fig. 4), which may be a conjugate structure in well-laminated rocks (Marshall, 1984).

S_2 is the hinge surface foliation of tight to isoclinal folds (F_2^0; see Fig. 5), and S_3 parallels the hinge surface of mesoscale folds which are parasitic upon the Joma Synform (F_3^{0-2}). The hinge surfaces of minor kinkbands, that overprint S_3, are designated S_4 and S_4'.

Orientation data for all the linear and planar fabric elements mapped at surface are shown in Fig. 6 (based on Odling, 1984; fig. 3). Disregarding the relatively uncommon D_4 structures, which have no significant effect on D_3 elements, F_3^{0-2} comprises tight to near-isoclinal folds of S_{0-2} with shallow SW-plunging hinge lines and moderate to steep NW-dipping hinge surfaces. The great-circle dispersion of D_3 hinge-line data is consistent with some variation in S_{0-2} orientation pre-D_3. Linear data for D_2, comprising F_2^0 hinge lines and a mostly co-linear mineral lineation, define an arc. Various factors, such as local divergence between F_2^0 and the mineral lineation, plunge variation of F_3, and inhomogeneous flattening accompanying F_3, impede interpretation of the redistribution pattern. However, consistent with the morphology of F_3 mesofolds, the pattern fits best a large (60–90°) small-circle distribution centred on F_3 and modified by inhomogeneous pure shear. Allowing that S_{0-2} dipped shallowly

Fig. 4. S_{0-2} in quartzose phyllites overprinted by an inhomogeneously-developed crenulation foliation S_3.

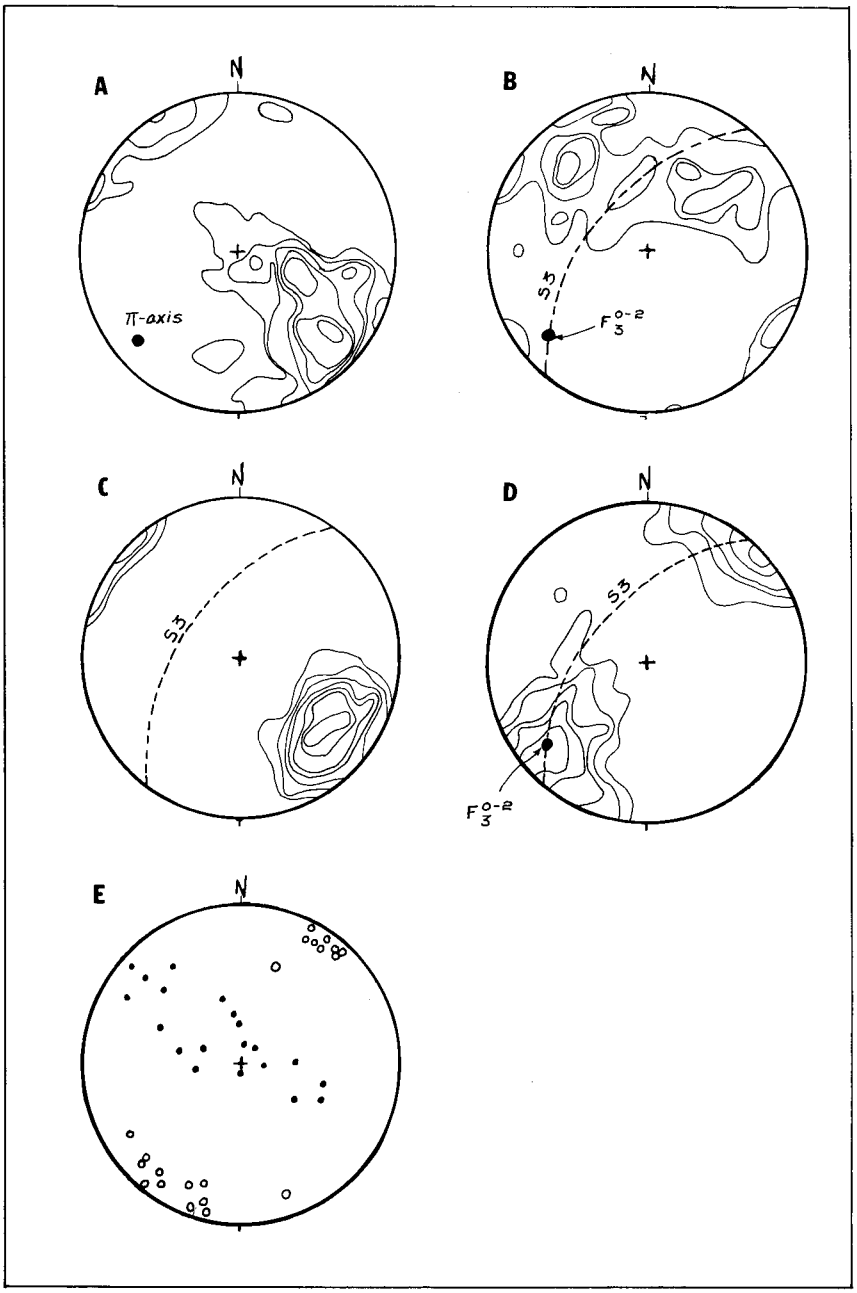

Fig. 6. Orientation data from surface exposures for planar and linear fabric elements from the Joma Mine area, modified from Odling (1984). Data are plotted on Lambert equal-area stereonets and contoured at 1-2-4-6-8-9+% per 1% area. Planar elements are plotted as poles.

(A) Transposition foliations (S_{0-2}): 243 data points defining a great circle distribution with Π-axis ($\equiv F_3^{0-2}$) plunging 18/230°.

(B) Mineral lineation (L_m) and co-linear F_2 hinge lines: 146 data points (125 L_m, 21 F_2); F_3^{0-2} and S_3 are based on Figs. 6A, C and D.

(C) Crenulation foliation (S_3) and F_3^{0-2} hinge surfaces: 139 data points; the maximum concentration suggests that regional S_3 dips 56/306°.

(D) F_3^{0-2} hinge lines and associated co-linear intersection and crenulation lineations: 147 data points; the maximum concentration is consistent with regional F_3^{0-2} plunging shallowly SW (cf. Fig. 6A). Minor non-cylindricality is reflected by dispersion within the S_3 great circle (from Fig. 6C).

(E) Hinge line and hinge surface elements ascribed to D_4.

TABLE 3

Fabric catalogue — mesoscale elements

Deformation		Form surfaces	Folds formed	Elements generated	Comments
D_1		S_0	No elements proved to belong to D_1 S_s in part pre-S_2 but not provably pre-D_2		
D_2	*Early*	S_0, S_b	?	S_s	not all S_s generated
		S_0, S_b	Group 1:	$S_2\, L_m$	$F_2^0//F_2^b//L_2^0$
		S_s	$F_2^0\, F_2^b$	$L_2^0\, L_2^s$	L_2^s//to sub//L_2^0
				$S_{0\text{-}2}\, S_{s\text{-}2}$	} Transposition foliations
			F_2^s	$S_{b\text{-}2}$	
	Late	not pertinent		S_s reactivated and extended (?) — new slides form	
D_3	*Strong*	$S_{0\text{-}2}$	Group 2:	$S_3\, S_c$	S_0 etc. included in transposition foliations
		$S_{s\text{-}2}$	F_3 in all form	L_c	
		$S_{b\text{-}2}$	surfaces		$S_3//S_c$
		S_2			$F_3//L_c$
	Weak	as above	Group 2:	$S'_3\, S'_c$	$S'_3//S'_c$
			F'_3 in all form surfaces	L'_c	$F'_3//L'_c$
D_4		as above plus S_c		S'_c is not a significant form surface Faulting - possible folding and crenulation, but data sparse - could be S'_3	

fabric elements are in Fig. 11. Stereograms were firstly compiled for the discrete elements on each level (e.g. S_0 separate form S_s) and then, if shown to have the same distribution, assembled into composite plots (e.g. $S_0+S_s+S_b$). The level data for these composite diagrams were subsequently compiled into synoptic diagrams for the mine (e.g. Fig. 11A).

Nothing in the subsurface distribution of D_4 structures suggests a significant redistribution of D_3 elements. F_3 may therefore be interpreted in terms of a moderately steep NW-dipping hinge surface, and a SW-trending subhorizontal hinge line with a tendency towards a hinge-surface-related great circle dispersion (Figs. 11F, H). As with the surface data (see above), the non-cylindricality is at least partly consistent with development of F_3 in a non-planar form surface; but, as indicated below, this is not the sole cause. The NW–SE trend in Fig. 11F results from S_3 shallowing as it passes from silicate hostrocks into massive sulphides. (This tendency is well illustrated by Figs. 11G and 12). Partly in conjunction with the decrease in hinge-surface dip, hinge lines rotate from NE–SW towards more northerly and westerly trends (Fig. 11H), although some non-cylindricality is still evident for steeply dipping hinge surfaces. Shallowing of hinge surfaces and concurrent rotation of hinge lines, as F_3 passes from silicate into sulphide rocks, is consistent with shear strains partitioning into sulphides.

Despite the abundance of D_3 mesofolds, synoptic S_{sob} and S_2 (Figs. 11A, B) show no indication of redistribution by a NE-trending F_3 (cf. Fig. 6A). This is consistent with data coming

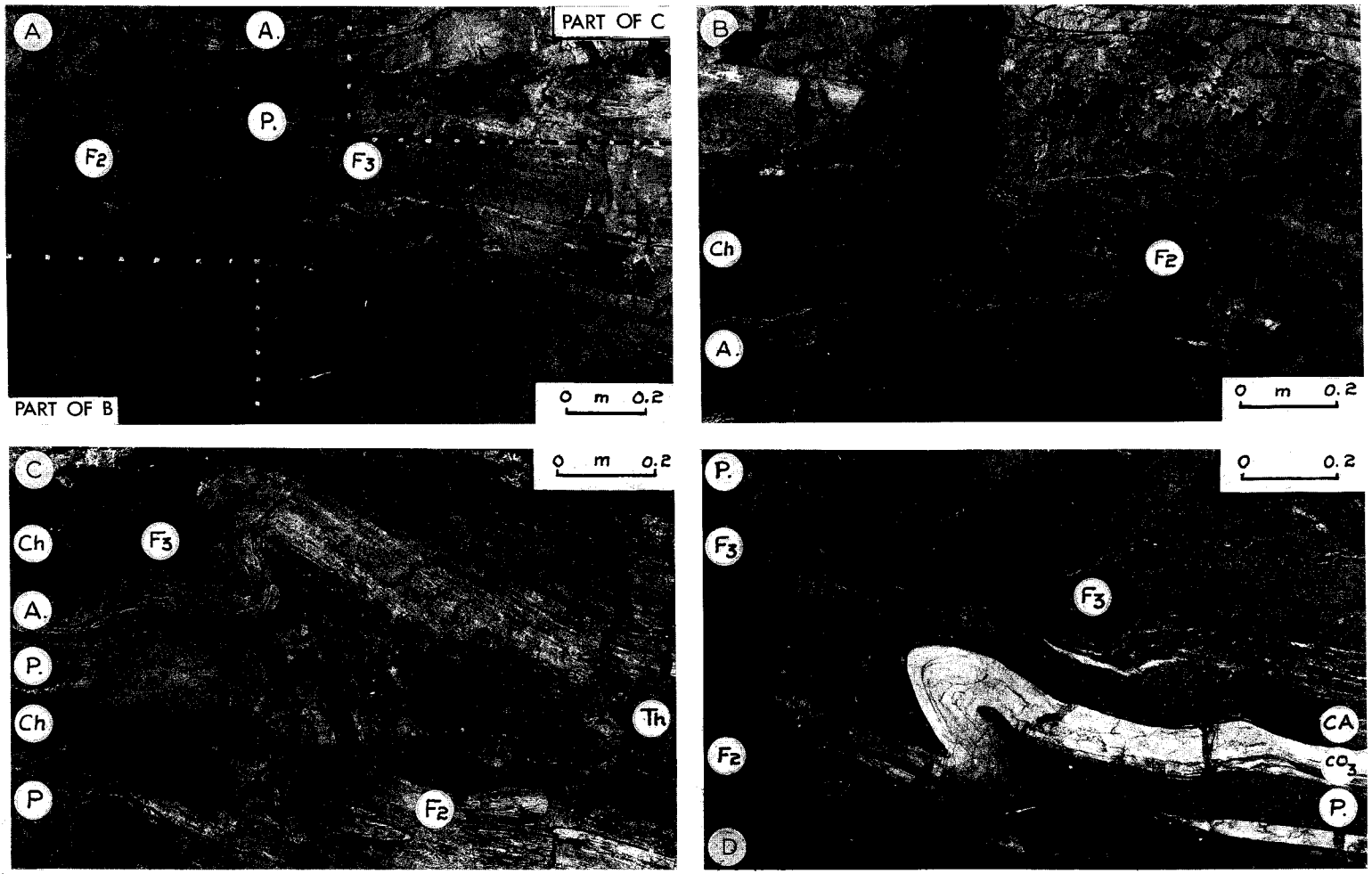

Fig. 9. F_2^0 folds in sulphides and intercalated layers of silicate rock: letter symbols as for Fig. 8.

(A) F_2^0 in chlorite schist in pyritic ore, overprinted by a more steeply dipping F_3^{0-2} flexure. The fields of B and C which partly overlap A are indicated.

(B) F_2^0 in albite laminite and chlorite schist; the upper limb has been sheared out against sulphides in which smaller F_2^0 isoclines are visible.

(C) F_2^0 in laminae of the albite laminite; the laminite layer is folded by a larger F_2^0 structure which has been thrust out along its hinge surface. An F_3^{0-2} fold is developed in the upper limb of the disrupted Z-fold.

(D) F_2^0 and F_3^{0-2} in carbonate/chlorite schist layers in pyrrhotite-rich sulphides. Note the attenuated lower limb of the F_2^0 isocline.

rotated during thrusting towards parallelism with L_m.

The subsurface fabric catalogue (Table 3) and orientation data (Fig. 11) are therefore consistent with two main periods of folding (F_2 and F_3) and one minor period (F_4; cf. Olsen, 1980; Odling, 1986; Marshall et al., 1987). They provide insight into the reorientation of F_2 and F_3 elements by thrusting and, as a consequence of folds passing from silicate rocks into massive sulphides, by a form of refraction. They also suggest that a significant thrusting or sliding episode pre-dated S_2 development, and this raises the possibility of a D_1 event with an associated phase of folding (F_1). These ideas, together with an indication of the amount of supporting evidence, are summarized as a deformation-event sequence (Table 4).

Vergence considerations

Vergence mapping is fraught with difficulty due to conjugate folds produced in D_3, the possible presence of D_4 folds, the inadequacy of orientation data as an absolute means of discriminating between F_2 and F_3, and the particular difficulty of distinguishing F_2 from F_3 folds in sulphide rocks where silicate foliations and lineations are not evident. Nevertheless, mapping of F_2 and F_3 vergence has provided important constraints on regional and mine scale structure.

At surface, based on the author's observations and on mapping by Odling (1984), F_2 vergence data in quartz-rich phyllites on both limbs of the Joma Synform indicate consistently that the region is positioned on the upper limb of a NE-closing F_2 antiform. If regional stratigraphy is inverted, as proposed by Kollung (see above), the vergence data require that inversion pre-dated F_2. However, at mine scale, the present study and previous investigations (Odling, 1984; Reinsbakken, 1986, fig. 32) are consistent with the position of the orebody being on the lower limb of a NE-closing F_2 antiform and thereby, based on the proposed regional in-

TABLE 4

Deformation sequences - mesoscale evidence

Event	Component event		Support
D_1	(a)	Isoclinal, large amplitude	Very weak at mesoscale
	(b)	Thrusting along and shallowly oblique to S_0 forming imbricate stacks	Strong but D_1 age not proved
D_2	(a)	As in (b) above - (b) and (a) are alternatives	Strong for pre-S_2
	(b)	Tight to isoclinal folding with short limbs exceeding 30m in level scale folds	Very strong
	(c)	Sliding along old and newly formed surfaces	Strong
D_3	(a)	Folding with close to isoclinal styles and moderate to shallow NW dipping hinge surfaces	Very strong
	(b)	Thrusting along old (?) and newly formed surfaces	Strong
	(c)	Folding with open to close styles and moderate to steep SE dipping hinge surfaces	Limited
	(d)	Relaxation faulting and development of dilation veins - NW dips for both structures	Weak
D_4	(a)	As above in (d) - (d) and (a) are alternatives	Weak
	(b)	Folding with open style and shallow SE dipping hinge surfaces	Very weak

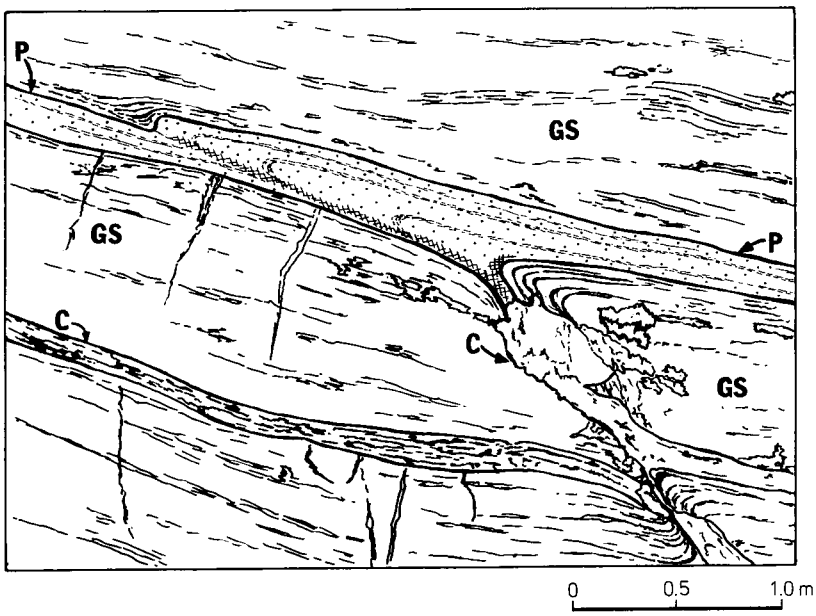

Fig. 12. Refraction (shallowing) of the F_3 hinge surface as it passes from thinly-layered greenstone into a layer of banded pyritic ore. In the pyritic ore, the hinge surface is marked by segregation of pyrrhotite-chalcopyrite (cross-hatched symbol). GS = greenstone, C = carbonate and P = pyritic ore.

version, being the correct way-up. These relationships, which conflict with proposals (e.g. Olsen, 1980; Reinsbakken, 1986) that the orebody stratigraphy is inverted, will be discussed later in this paper.

F_3 vergence varies regionally across the hinge surface of the Joma Synform, and this geometry is largely supported at mine scale. Mesoscale vergence has either a hinge zone "M" geometry, as at the north end of the open cut (560 level), or a lower limb "S" geometry (looking SW) in all subsurface levels investigated. Thus,

Fig. 11. Orientation data of planar and linear fabric elements from Joma Mine. Data are plotted on Lambert equal-area stereonets; planar elements are plotted as poles.

(A) Synoptic S_{s0b}, a composite plot of $S_0+S_s+S_b$ from all mapped levels: 230 poles contoured at 1-3-6-9-12% per 1% area; the partial girde distribution defines πS_{s0b} ($\equiv F_2$) as 20/302°.

(B) Synoptic S_2: 72 poles contoured at 1-3-7-10% per 1% area. The weak partial girdle defines πS_2 as 22/324°. The statistically defined S_2 (equivalent to the maximum concentration of S_2 poles) dips 22/324°.

(C) Synoptic F_2+L_2: 113 data points contoured at 1-3-5-8-11% per 1% area. The S_2 great circle is from Fig. 11B. The maximum concentration plunges at 20/311°.

(D) Synoptic L_m: 93 data points contoured at 1-4-7% per 1% area. The S_2 great circle is from Fig. 11B. The maxima plunge 20/320° and 25/340°.

(E) Synoptic stereogram of D_2 linear elements comprising $F_2+L_2+L_m$: 206 data points contoured at 1-3-6-8% per 1% area. The maximum concentration plunges at 23/320°. The best-fit great circle ($=S_2$) dips 23/305°.

(F) Synoptic stereogram of D_3 planar elements comprising S_c and F_3 hinge surfaces. Circles are S'_c: 184 poles contoured at 1-3-6-9-12% per 1% area. The statistically defined S_c dips 50/318°.

(G) Crenulation foliation (S_c) and F_3 hinge surfaces from level 387 (located on Fig. 7): 73 poles contoured at 1-5-9-12-15% per 1% area. Concentrations 1 and 2 are, respectively, from silicate and sulphide rocks and dip 54/325° and 24/332°.

(H) Synoptic stereogram of D_3 linear elements comprising L_c and F_3 hinge lines. Circles are L'_c: 214 data points contoured at 1-2-4-7-10% per 1% area. Great circles 1 and 2 (delimiting a suite of great circles that could be fitted to the data) dip 80/312° and 22/330° and are, respectively, equated with silicate and sulphide rocks.

TABLE 6

The principal sulphide rock units (ore type)

Units (ore types)	Subdivisions (ore subtypes)	Comments
Zinc-rich pyritic ore (A)	Banded sphalerite ore (BS)	Fine- to medium-grained pyritic ore, expressing recrystallization banding; contains carbonate as matrix, streaks and more continuous layers; sphalerite-rich layers (<5 mm up to 50 mm) are variably spaced throughout; a variant with silica instead of carbonate is similar to BQC (below)
	Massive medium-coarse grained ore (MMG)	Pyritic ore with variable amounts of carbonate matrix and disseminated sphalerite; gradational into BS as layering becomes more obvious and the sphalerite content increases
	Banded to massive, medium grained ore (BMG)	Pyritic ore with pyrrhotite and variable amounts of sphalerite and/or chalcopyrite
Copper-rich pyritic ore (B)	Banded actinolite-rich ore (BA)	Fine- to medium-grained banded (on a scale of 0.25 to 1.5 cm) pyrite-pyrrhotite-chalcopyrite ore; alternate bands consist of layers (probable bedding) of richly disseminated actinolite (?) needles; magnetite layers also present
	Banded quartz-carbonate ore (BQC)	Fine- to medium-grained pyrite with pyrrhotite and chalcopyrite displaying recrystallisation banding up to 3 cm thick; associated with discontinuous layers and streaks of grey-black chert-like quartz and carbonate, and uncommon magnetic layers
Copper/zinc-poor pyritic ore (C)	Massive actinolite-rich ore (MA)	Fine-grained pyritic ore with disseminated oriented/disoriented actinolite(?) needles; with decreasing actinolite it is transitional into MFG (below); with increasing pyrrhotite-chalcopyrite it is transitional into ore-type D (below)
	Massive fine-grained ore (MFG)	Very fine- to fine-grained flinty pyrite with minor amounts of zinc and copper; is brecciated and healed with diffuse-margined veins of medium-grained pyrite; lacks a carbonate matrix; transitional into MMG
	Banded fine-grained ore (BFG)	Layers (<1 cm up to 20 cm) of very fine-grained and fine-grained flinty pyrite with breccia veining; transitional into MFG and with increasing matrix carbonate, into A ore-types
Chalcopyrite-pyrrhotite ore (D)	Banded to massive ore (BM)	With increasing chalcopyrite and pyrrhotite contents, the B ore-types develop thin and segregations of chalcopyrite-pyrrhotite mineralisation; also see the MA sub-type (above)
	Durchbewegt ore (DB)	Further increase and segregation of chalcopyrite and/or pyrrhotite results in layers and masses of chalcopyrite-pyrrhotite ore containing angular to subrounded pieces of once continuous layers of silicate rock, vein quartz and pyritic ore

Silicate rock units (Table 5)

Types 1 and 2 greenstone are believed to represent pre- and post-ore metavolcanites, respectively (cf. Olsen, 1980; Reinsbakken, 1986), principally because type 1 carries disseminated and stringer pyrite and is more altered. In other respects, such as the presence of small pillow and pillow-breccia horizons associated with thinly layered tuffs(?), the two types are similar, although Reinsbakken reported significant differences in TiO_2 and Zr contents.

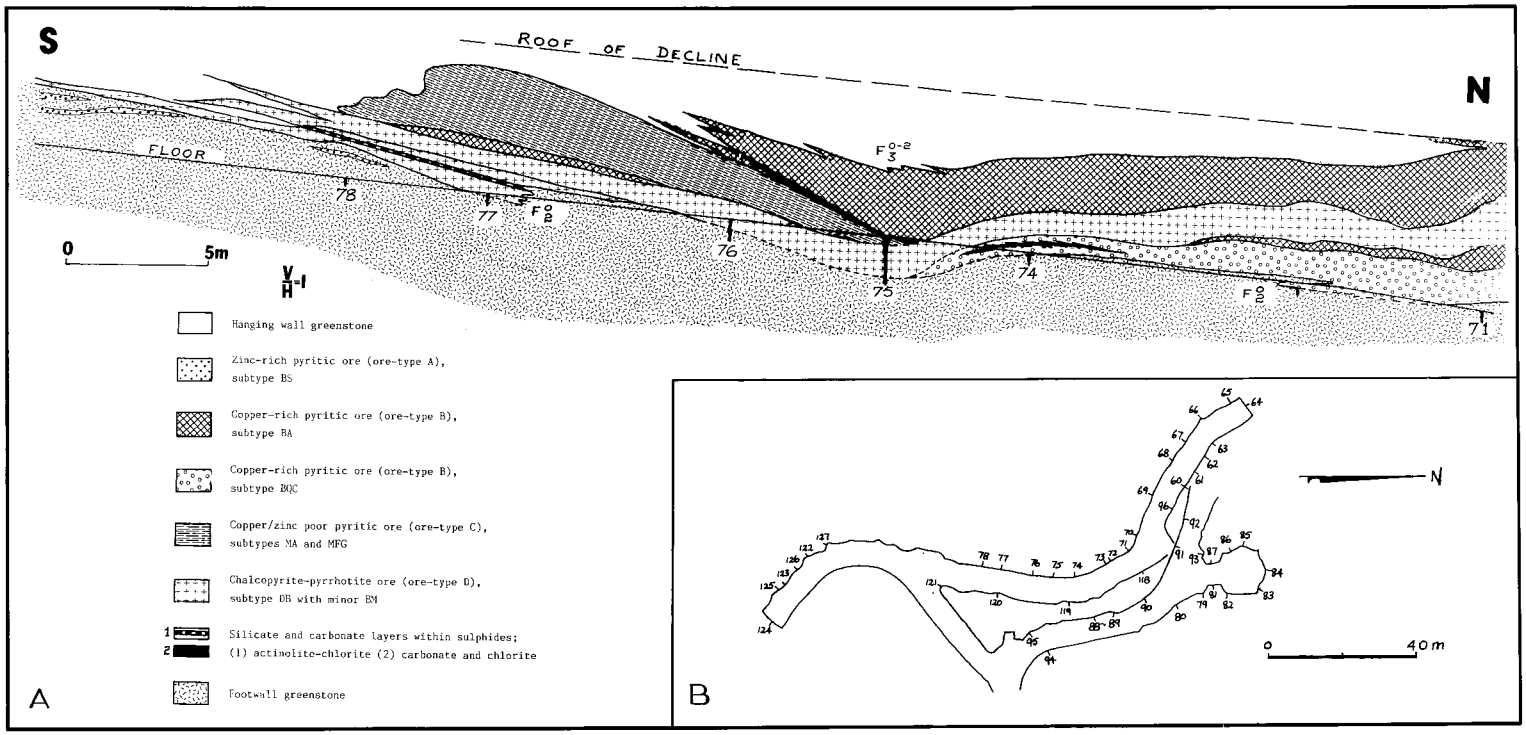

Fig. 13. Ore-layer sequence and locality plan, level 375 decline. (A) Simplified section of the ore-layer in the W wall. Refer to Tables 5 and 6 for amplification of the legend. (B) Locality plan of the 375 decline and portion of level 375 (see Fig. 7).

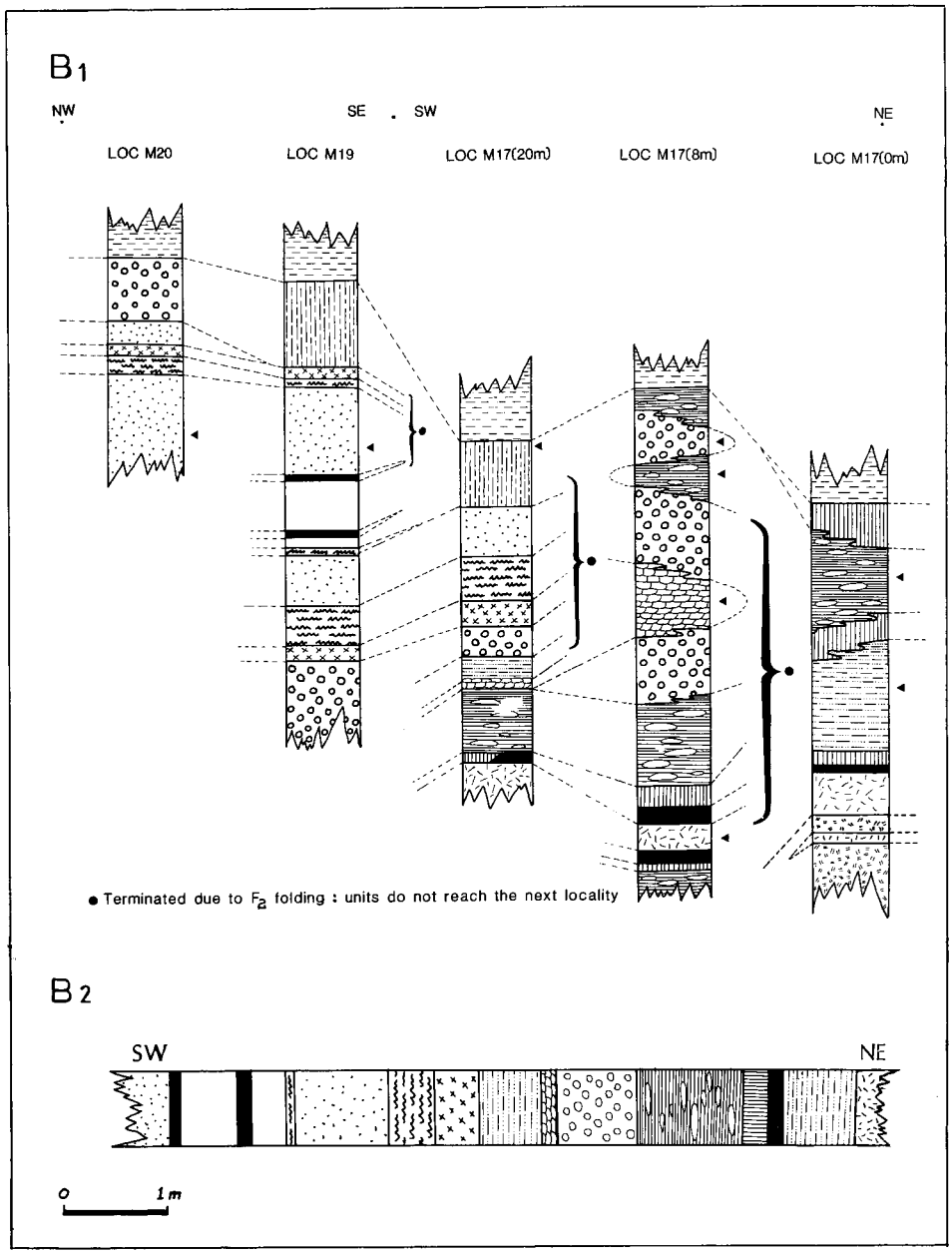

Fig. 14B. Caption see Fig. 14C.

hangingwall to footwall in level 375 decline, and levels 387 and 495 (located on Fig. 7), are presented in Figs. 13, 14 and 15, respectively. Where F_2 and F_3 folding have influenced the sequence, this is either shown on the section or the effect has been removed. Contacts clearly of tectonic origin are also shown on the section.

The ore-layer sequences from these and other mapped levels are summarised in Table 4, and collectively portray the following principal characteristics:

(a) Although individual layers may be lenticular or wedge out, and others (particularly silicate rock intercalations involving Abl

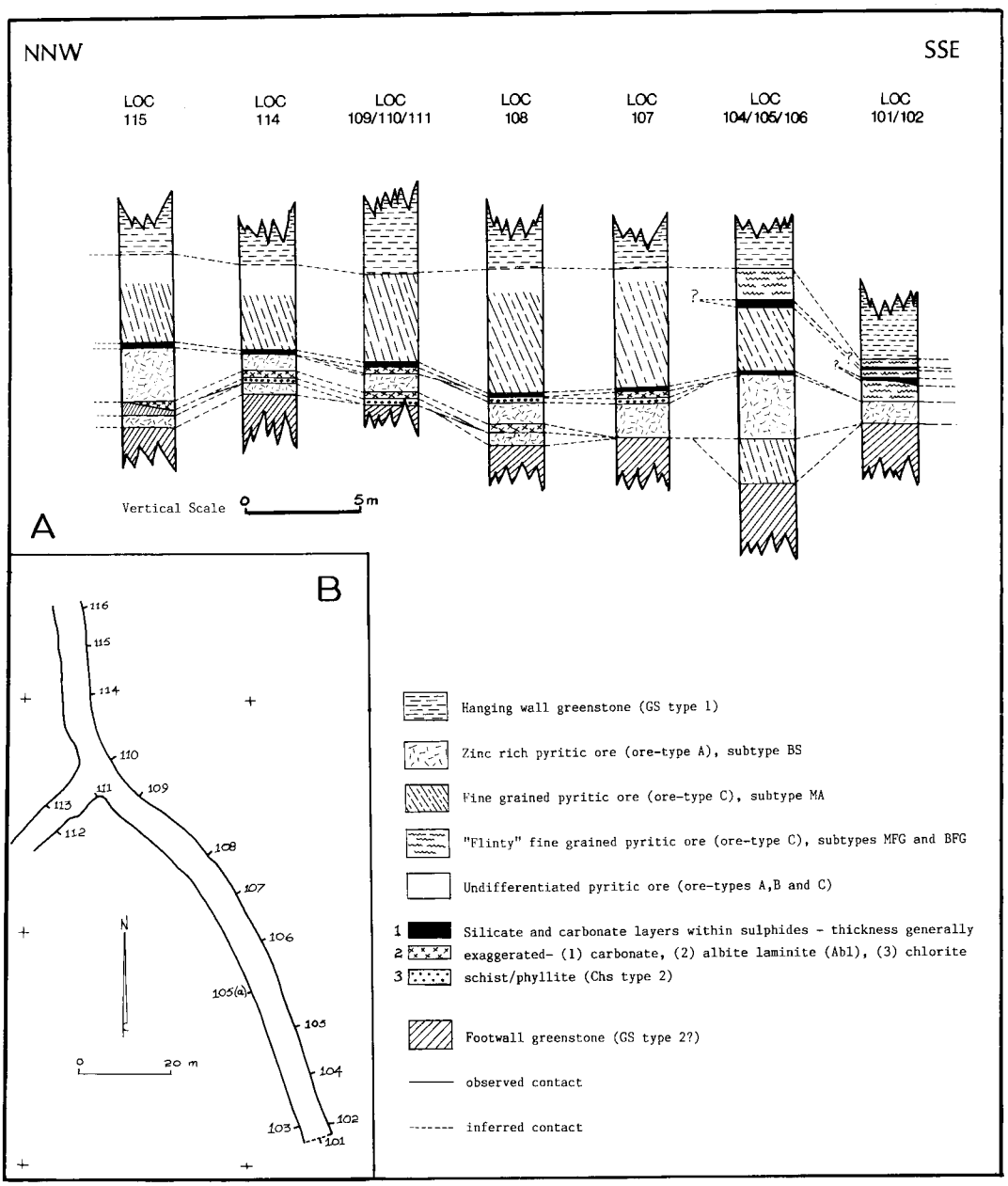

Fig. 15. Ore-layer sequences and locality plan, level 495. (A) Sequences from hangingwall to footwall at designated localities. Refer to Tables 5 and 6 amplification of the legend. (B) Plan of S end of level 495 (see Fig. 7) showing localities in Fig. 15A.

and Chs type 2) may be repeated with constant polarity (Fig. 16), a reasonably consistent sequence can be mapped throughout substantial portions of a given level (Figs. 14, 15).

(b) Despite parts of the sequences being common to several levels, there is no obvious sequence common to all mapped levels; that is, the order of rock units is inconsistent.

TABLE 7

Ore-layer sequence in selected levels of Joma mine

Level	560	495	387	375	375 decline	362
Hanging wall	*GS type 1; pillow lavas, sulphide veins and disseminations	GS type 1(?)/ Chs type 1 "transition" rocks	GS - well layered but of uncertain type	GS - well layered and pale chlorite-rich - type 2(?)	GS - pale chlorite-rich - type 2 affinity	GS - well layered but type uncertain
	Abl/minor Abt/Abp grading to Chs type 2	MA/MFG with CO_3 layers and Chs type 3	MFG/MFG with CO_3 layers - pyrrhotite-rich in places	BFG/BA	BA/BFG/MA	MFG/BFG
	MA/BA/MMG with minor BS and CO_3 layers	Chs type 2 over CO_3 + Chs type 3 + Abl	BM/DB	MFG	BMG/DB at various levels	BS
	MFG/BFG/ MMG	BS	Chs type 2	BA/BFG	BA/BQC	Dark green chlorite schist - Chs type 1(?)
	BS	Abl/Abp over Chs type 2	Abl	DB but position varies	MFG/DB	
	GS type 2; well-layered tuffs and pillow lavas - no sulphides	BS	MA/MFG/BMG	BQC over BS	Chs type 1/GS type 1/CO_3 rich GS	
		MA	Chs rich in actinolite - type 1(?)	Chs type 1 and dark-chlorite GS - type 1(?)		
		Abp/Chs type 3/ GS (type uncertain but suspect 2)	BMG/BQC/BS			
			Chs type 1/GS type uncertain - type 1(?)			
Footwall						
Exploited thickness	25–30 m	~7.0 m	~7.0 m	4.5–7.5 m		~15 m

*No lateral correlation is implied between units; abbreviations as in Tables 5 and 6.

(a) S_2, which constitutes the tectonic contacts between different units in the ore-layer sequences in Table 7, being overprinted by S_2 in F_2 hinge zones.

(b) S_s being form-surface to F_2 folds. This is well illustrated by a large F_2 fold (Fig. 17) from level 387; the pseudostratigraphy (S_s), which characterises much of level 387 (Fig. 14B, Table 7), clearly developed before F_2.

It now remains to consider whether the event which generated the pseudostratigraphy (S_s) solely involved thrusting (compatible with early-D_2 or D_1 possibilities), or folding and thrusting (only compatible with a D_1 event).

Evidence for D_1 folding and thrusting

Limited support for a D_1 event is provided by sparse microfabric data, inter-regional comparison of deformation-event sequences, and the need to reconcile younging and vergence data. Each of these is considered below.

Microfabric data

Remnants of a rare pre-S_2 foliation are preserved in the noses of a few F_2 folds in layered metavolcanites. The pre-S_2 foliation is defined by a felt of fine-grained chlorite within thin (<2 cm) layers. The layers are slightly crenulated

TABLE 8

Inter-regional "equivalence" of deformation/fold events - Joma and adjacent regions

Kollung (1979)	Lutro (1979)	Roberts (1979)	This article	Zachrisson (1969-'71)	Trouw (1973)	Sjöstrand (1978)
	D_0^*	pre-D_1^{**}	D_1	pre-F_1	F_1	D_1, D_2
F_1^{***}	D_1	D_1	D_2	F_1	F_2	D_3
F_2^{****}	D_2	D_2	D_3	F_2	F_3	D_4
F_{2a}	D_3	D_3		F_3	F_4	D_5
	D_4		D_4			
F_3	D_5'	D_4				

*Of restricted distribution.
**Known from outside the area mapped but of limited significance.
***Event producing the principal foliation and mineral lineation.
****The Joma Synform (Kollung, 1979) and Ransaren or Eastern Synform (Zachrisson, 1969; Trouw, 1973).

ing is an assumption based on inversion of the Limingen and Gjersvik Groups in the structurally overlying Limingen Nappe (Kollung, 1979), and on Kollung's extensive experience in the Central Norwegian Caledonides. The author's knowledge of the region is insufficient to evaluate the assumption, which must necessarily detract from the argument for F_1 based on opposed vergence. In relation to (b), conclusive support for F_1 would come from opposed-facing within individual F_2 folds, but younging data are extremely scarce. On a regional basis, Kollung (1979) cited an example from pillow lavas and one case of graded bedding. In the mine district, despite the abundance of small pillows, the evidence was inconclusive, because the development of secondary cusps (during D_3) at pillow interfaces precludes unambiguous interpretation.

Reconciliation of vergence data with published stratigraphic facing clearly requires an F_1 event, but inability to substantiate published facing by younging data means that F_1 remains contentious.

Conclusion

Although there is no mesoscale evidence exclusively favouring D_1, there is incontrovertible evidence for a pre-S_2/pre-F_2 thrusting event. Inconclusive support for an F_1 event with which the pre-F_2 thrusting could be associated, is provided by three lines of evidence (microfabric data, inter-regional comparison of event sequences, and interpretation of facing and vergence data); although weak individually, they collectively constitute a significant argument for a D_1 event.

Implications of mine-scale stratigraphy

Despite the existence of pseudostratigraphy at level scale, a systematic relationship between host rocks, wallrock alteration, and the main ore types at mine scale has been designated gross stratigraphy. Although parts of the sequence may be absent (cf. Figs. 3 and 18), the interpretation is consistent with popular models of volcanic-associated massive sulphide deposits (Franklin et al., 1981; Marshall and Gilligan, 1987) and has considerable appeal over the alternative view that the sequence is a thrust package lacking stratigraphic significance.

Of course, crude preservation of stratigraphic and genetic relationships does not preclude substantial distortion and disruption during folding and thrusting, but it does have implications regarding the scale of the structures. Thus:

does not, however, preclude folding at a much larger scale, as advocated by Kollung (1979).

Structural evolution of the orebody

The existence of primary layering within the orebody defined variously by silicate, magnetite, and quartz–carbonate laminae together with layers with different percentages of the principal iron, copper and zinc sulphides, supports a syn-sedimentary genesis. Bearing in mind the associated pillow lavas and tuffs, the hydrothermal alteration effects that are interpreted as a feeder system, and the grossly concordant tabulate geometry of the ore layer, it may be concluded that the massive sulphide deposit most probably formed by seafloor exhalative processes. Its original geometry and zonation most likely approximated Cu–Zn deposits of similar mafic volcanic affiliation. (See, for example, Vokes, 1976; Franklin et al., 1981; Stephens et al., 1984; Marshall and Gilligan, 1987.)

Because the orebody experienced all of the deformation events, the questions become to what extent and at what scale have these events modified original relationships? Particularly so, given Olsen's (1980) proposal (endorsed by Reinsbakken, 1986) that the relative position and bulk chemistry of original layers were maintained during deformation and metamorphism. The questions are partly answered under mine scale stratigraphy (above), but they will be more closely examined in the context of orebody evolution. The events will be discussed in their order of superposition.

The D_1 event

F_1 folding is required on a scale exceeding 650 m and probably 1200 m (current orebody dimensions), such that the orebody lies within a single limb. Small-scale folds were not observed and this, coupled with S_1 being weak to absent, suggests only small finite strains on the limbs of F_1. Given these circumstances, orebody relationships would have undergone negligible redistribution by folding.

In contrast, D_1 thrusting has induced pseudostratigraphy at level scale, but at mine scale it has produced neither gross repetition of the ore layer, nor dismemberment to a degree where the ore became isolated from the feeder system. These relationships are consistent with the ore layer being composed of a zone of shear displacements between relatively rigid plates of hangingwall and footwall greenstone. The sense of displacement could not be determined, but translation from NW to SE is favoured by the possibility that D_1 and D_2 are kinematically similar. At the end of D_1, allowing that F_1 produced recumbent folds, the thrust-disrupted ore layer would have occupied the upper limb of a regionally developed E-closing antiformal anticline.

The D_2 event

F_2 produced the principal schistosity and mineral elongation lineation, and folded the ore on scales ranging from a few centimeters upto a hundred meters in amplitude. It also folded regional F_1 into an E-closing, near recumbent, antiform of regional dimensions, thereby inverting the ore layer and ensuring the appropriate distribution of younging and vergence. The near isoclinal to isoclinal folds have thickened disrupted hinge zones and highly-attenuated sheared-out limbs. Hinge-line orientations rotated towards parallelism with the SE-trending elongation fabric during general thrust translation from NW to SE. According to Vokes (1986) F_1 and F_2 fold systems are probably coaxial.

Thrusting and sliding accompanied F_2 and probably reactivated some of the D_1 tectonic surfaces. They also disrupted the ore layer and formed level-scale ellipsoidal bodies with long axes paralleling the local hinge-line orientation.

Despite the extreme distortions accompanying D_2, gross relationships between ore layer and feeder system were apparently preserved. Thus, at the end of D_2, the downward younging and

acteristics in the ore where the sulphides act as a décollement layer between hanging wall and footwall silicate rocks, typify deposits in thrust and nappe tectonic regimes.

Acknowledgements

Professor Frank Vokes (University of Trondheim) and Arve Haugen (Grong Gruber A/S) made this work possible. I am most grateful for their support and for the support of their respective organisations. Arne Reinsbakken, Noelle Odling and Wilfried Liessmann were concurrently working at Joma Mine; they freely exchanged ideas during stimulating and sometimes heated discussions. A travel grant in support of this study program was provided by the New South Wales Institute of Technology.

Frank Vokes, Noelle Odling, Lindsay Gilligan and Mike Stephens read the typescript and made useful suggestions regarding its improvement. Two anonymous referees are thanked for their contributions. Nonie Green patiently drafted the figures and Vi Searle did the typing.

The paper was verbally presented at the International Conference on Rock Deformation held at Mt. Buffalo, Victoria (Australia) in February, 1987.

References

Bell, T.H. and Rubenach, M.J., 1983. Sequential porphyroblast growth and crenulation cleavage development during progressive deformation. Tectonophysics, 92: 171–194.

Bjørlykke, A., Grenne, T., Reinsbakken, A. and Vik, E., 1979. Compilation of stratabound sulphide deposits in the Norwegian Caledonides. Nor. Geol. Unders., Rep. 27, 20 pp.

Bjørlykke, A., Grenne, T., Rui, I. and Vokes, F.M., 1980. A review of Caledonian Stratabound Sulphide deposits in Norway. Geol. Surv. Ireland, Spec. Pap. 5: 29–46.

Breitkoff, J.H. and Maiden, K.J., 1988. Tectonic setting of the Matchless Belt pyritic copper deposits, Namibia. Econ. Geol., 83: 710–723.

Burns, K.L., Shepherd, J. and Marshall, B., 1978. Analysis of relational data from metamorphic tectonites; derivation of deformation sequences from overprinting relations. In: D.F. Merriam (Editor), Recent Advances in Geomathematics. Pergamon, New York, N.Y., pp. 171–199.

Davis, G.H., 1972. Deformational history of the Caribou stratabound sulfide deposit, Bathurst, New Brunswick, Canada. Econ. Geol., 67: 634–655.

Franklin, J.M., Lydon, J.W. and Sangster, D.F., 1981. Volcanic-associated massive sulphide deposits. Econ. Geol., 75th Anniv. Vol.: 485–627.

Gaal, G., 1977. Structural features of Precambrian stratabound sulphide-ore deposits in Finland. Geol., Gören. Stockholm Förh., 99: 188–126.

Gee, D.G. and Roberts, D., 1983. Timing of deformation in the Scandinavian Caledonides. In: P.E. Schenk (Editor), Regional Trends in the Geology of the Appalachian-Caledonian-Hercynian-Mauritanide Orogen. Reidel, Dordrecht, pp. 279–292.

Gilligan, L.B. and Marshall, B., 1987. Textural evidence for remobilization in metamorphic environments. Ore Geol. Rev., 2: 205–229.

Halls, C., Reinsbakken, A., Ferriday, I., Haugen, A. and Rankin, A., 1977. Geological setting of the Skorovas orebody within the allochthonous volcanic stratigraphy of the Gjersvik Nappe, central Norway. Geol. Soc. London, Spec. Publ., 7: 128–151.

Klau, W. and Large, D.E., 1980. Submarine exhalative Cu-Pb-Zn deposits, a discussion of their classification and metallogenesis. Geol. Jahrb., Sec. D., 40: 13–58.

Klemd, R., Maiden, K.J. and Okrusch, M., 1987. The Matchless copper deposit, southwest Africa/Namibia: a deformed and metamorphosed massive sulfide deposit. Econ. Geol., 82: 587–599.

Kollung, S., 1979. Stratigraphy and major structures of the Grong district, Nord-Trondelag. Nor. Geol. Unders., 354: 1–51.

Krebs, W., 1981. The geology of the Meggen ore deposit. In: K.H. Wolf (Editor), Handbook of Stratabound and Stratiform Ore Deposits, Vol. 9. Elsevier, Amsterdam, pp. 509–549.

Laznicka, P., 1985. Concordant versus discordant ore deposits and ore transformations. In: K.H. Wolf (Editor), Handbook of Stratabound and Stratiform Ore Deposits, Vol. 11. Elsevier, Amsterdam, pp. 119–316.

Lister, G.S. and Williams, P.F., 1983. The partitioning of deformation in flowing rock masses. Tectonophysics, 92: 1–34.

Lutro, O., 1979. The geology of the Gjersvik area, Nord-Trondelag, Central Norway. Nor. Geol. Unders., 354: 53–100.

Marshall, B., 1984. First Progress Report: Joma Project. Report to Grong Gruber A/S October 1. 11 pp. (unpubl.).

Marshall, B., 1988. The interpretation of durchbewegung structure, piercement cusps and piercement veins. Geol. Soc. Aust., Abstr., 21: 282–283.

Marshall, B. and Gilligan, L.B., 1987. An introduction to remobilization: information from ore-body geometry and experimental considerations. Ore Geol. Rev., 2: 87–131.